

Chlorine (^{35}Cl) MRI in Humans: Cl^- Alterations do not Correspond to Disease-Related Na^+ Changes

Armin M. Nagel¹, Marc-André Weber^{2,3}, Frank Lehmann-Horn⁴, Karin Jurkat-Rott⁴, Alexander Radbruch^{3,5}, Reiner Umathum¹, and Wolfhard Semmler¹

¹Dpt. of Medical Physics in Radiology, German Cancer Research Center (DKFZ), Heidelberg, Germany, ²Dpt. of Diagnostic and Interventional Radiology, University Hospital of Heidelberg, Heidelberg, Germany, ³Dpt. of Radiology, German Cancer Research Center (DKFZ), Heidelberg, Germany, ⁴Division of Neurophysiology, Ulm University, Ulm, Germany, ⁵Dpt. of Neuroradiology, University Hospital of Heidelberg, Heidelberg, Germany

Target Audience: Scientists and physicians interested in the field of non-proton MRI

Purpose: Chlorine (Cl^-) is the most abundant anion in the human body and is involved in many physiological processes. Cl^- channels of the cell membrane contribute to volume regulation, ionic homeostasis, transepithelial transport and regulation of electrical excitability [1]. Skeletal muscle exhibits a very high Cl^- conductance [2]. Thus, the resting potential of muscle cells can be estimated from the intra- and extracellular Cl^- concentration. Studies with human chondrocytes indicate that their proliferation is linked to the membrane potential [3]. Cl^- channels also play a crucial role in glioma cell migration and invasion [4]. Therefore, the non-invasive measurement of the cellular Cl^- concentration and distribution is highly desirable and might provide insights into patho-physiological processes of several diseases. ^{35}Cl MRI has been applied for small animal imaging [5] and recently we demonstrated its feasibility for imaging of the healthy human muscle and brain [6]. In this work we present first results for the visualization of patho-physiological processes in humans.

Methods: ^{35}Cl MRI was conducted on a 7-T whole-body MR system (MAGNETOM 7 T, Siemens AG, Healthcare Sector, Erlangen, Germany) using a dual tuned ($^1\text{H}/^{35}\text{Cl}$), quadrature birdcage coil (inner coil diameter: 22 cm) (QED, Mayfield Village, Ohio, USA). To evaluate if ^{35}Cl MRI can yield additional information to established techniques, ^{23}Na MRI was performed using a dual tuned ($^1\text{H}/^{23}\text{Na}$) quadrature birdcage coil (Rapid Biomed GmbH, Rimpar, Germany). All ^{23}Na and ^{35}Cl MRI sequences were based upon a density-adapted 3D radial projection reconstruction pulse sequence [7]. Signal intensities were normalized to reference tubes containing saline solution and agar gel. Additionally to the 7 Tesla MR data, ^1H MRI data acquired at a 3 Tesla were available. To evaluate the feasibility of ^{35}Cl MRI to visualize patho-physiological processes, results from one patient with a confirmed glioblastoma, one enchondroma of the left distal femur and from one patient with a muscular ion channel disease (hypokalemic periodic paralysis) are presented.

Parameters Glioblastoma Patient (c.f. Fig. 1): To assess the local Cl^- concentration, relaxation weighting was minimized using a short echo time ($\text{TE} = 0.7$ ms) and a long repetition time ($\text{TR} = 65$ ms) (^{35}Cl conc.). Additional parameters: readout duration: $T_{\text{RO}} = 10$ ms; $\alpha = 90^\circ$; nominal resolution: $\Delta x^3 = (6 \text{ mm})^3$; Hamming filtering; acquisition time $T_{\text{acq}} = 9$ min 45 s. To suppress signal from Cl^- with longitudinal relaxation times like cerebrospinal fluid, an inversion recovery (IR) sequence was applied (^{35}Cl IR). Parameters: $\text{TE} = 0.8$ ms; $\text{TR} = 150$ ms; $\text{TI} = 24$ ms; $\Delta x^3 = (10 \text{ mm})^3$; $T_{\text{RO}} = 5$ ms; $T_{\text{acq}} = 10$ min. ^{23}Na MRI sequences with similar contrasts were applied. Parameters: ^{23}Na conc.: $\text{TE}/\text{TR} = 0.3/120$ ms; $T_{\text{RO}} = 10$ ms; $\alpha = 90^\circ$; $\Delta x^3 = (3 \text{ mm})^3$; Hamming filtering; $T_{\text{acq}} = 10$ min; ^{23}Na IR: $\text{TE} = 0.75/185$ ms; $T_{\text{RO}} = 10$ ms; $\Delta x^3 = (4.5 \text{ mm})^3$; $T_{\text{acq}} = 9$ min 52 s.

Parameters Enchondroma Patient (c.f. Fig. 2): ^{35}Cl MRI: $\text{TE}/\text{TR} = 0.35/60$ ms; $T_{\text{RO}} = 5$ ms; $\alpha = 90^\circ$; $\Delta x^3 = (6 \text{ mm})^3$; 3 averages; $T_{\text{acq}} = 30$ min. ^{23}Na MRI: $\text{TE}/\text{TR} = 0.4/101$ ms; $T_{\text{RO}} = 10$ ms; $\alpha = 90^\circ$; $\Delta x^3 = (6 \text{ mm})^3$; 3 averages; $T_{\text{acq}} = 30$ min 18 s.

Muscle-imaging (c.f. Fig. 3): ^{35}Cl MRI: $\text{TE}_1 = 0.35, 0.55, 0.75, 1.00, 1.25, 1.50, 2.75$ ms; $\text{TE}_2 = 4, 4.6, 5.2, 6.0, 6.6, 7.3, 8$; $\text{TE}_3 = 8, 9, 10, 11, 12, 13, 14$ ms; $\alpha = 90^\circ$; multi-echo sequences (5 min each); $\text{TR} = 60$ ms; $T_{\text{RO}} = 2.5$ ms; $\Delta x^3 = (11 \text{ mm})^3$. ^{23}Na MRI: $\text{TE} = 0.35$ ms; $\text{TR} = 160$ ms (93 ms); $T_{\text{RO}} = 10$ ms; $\alpha = 90^\circ$ (45°); $\Delta x^3 = (4 \text{ mm})^3$. Corrections for B_0 and B_1 inhomogeneities were performed.

Results: Concentration weighted imaging revealed increased ^{23}Na and ^{35}Cl signal intensities in enhancing and non-enhancing parts of the glioblastoma (Fig. 1). In IR imaging ^{23}Na and ^{35}Cl MRI showed opposed behavior (Fig. 1). Whereas large parts of the affected area exhibit decreased ^{23}Na IR signal, the ^{35}Cl IR signal shows a distinct increase (Fig. 1). ^{35}Cl and ^{23}Na MRI data of an enchondroma of the left distal femur are shown in figure 2. The measured chlorine concentration is approximately 7-fold lower than the sodium concentration. In muscle tissue of the patient with hypokalemic periodic paralysis, the measured Cl^- concentration is 1.5-fold smaller than the Na^+ concentration (Fig. 3).

Discussion and Conclusion: In this work ^{35}Cl images of different pathologies were acquired for the first time in humans. These preliminary results show different signal behavior for ^{23}Na and ^{35}Cl MRI, which demonstrates the fact that Cl^- does not only act as counterion for Na^+ . Thus, ^{35}Cl MRI can complement ^{23}Na MRI in clinical research and might enable a better analysis of (patho-) physiological processes in the future.

References: [1] Jentsch, *Physiol. Rev.* (2002) 82: p. 503; [2] Jurkat-Rott, Lehmann-Horn F, *In: Myology*, McGraw-Hill, 2004, pp. 203-231, [3] Wohlrab D, Hein W. *Orthopade* 2000; 29(2):80-84. [4] Olsen ML et al. *J Neurosci* 2003;23(13):5572-5582. [5] Kirsch S, et al. *NMR in Biomed* (2010) 23: p. 592; [6] Nagel AM, et al. *In Proc. ISMRM 2012*, p. 1699; [7] Nagel AM, et al. *MRM* (2009) 62: p. 1565

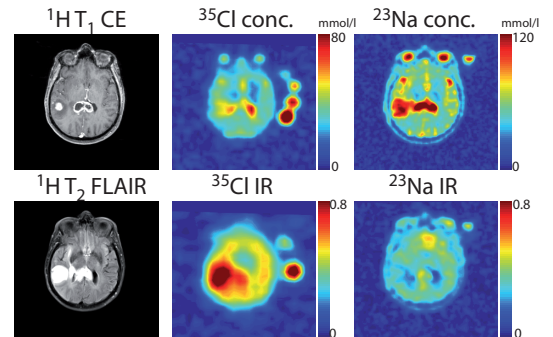


Fig. 1: Glioblastoma (WHO $^{\circ}\text{IV}$) of the right temporal lobe and the corpus callosum. ^{23}Na conc. MRI revealed elevated signal intensity in all parts of the tumor, whereas ^{23}Na IR showed parts with reduced and increased signal intensities. Slightly increased signal intensities are also visible in ^{35}Cl conc. MRI. In contrast to ^{23}Na IR imaging, ^{35}Cl IR MRI revealed a strong signal increase in the affected brain region.

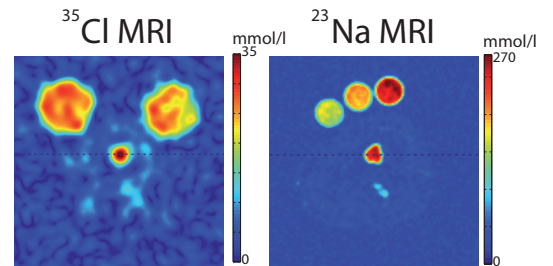


Fig. 2: Selected transversal slices of 3D ^{35}Cl and ^{23}Na data sets of an enchondroma patient. The measured Na^+ concentration (255 mmol/l) of the enchondroma is approximately 7-fold higher than the Cl^- concentration (36 mmol/l). Note the excellent tumor delineation from normal bone marrow.

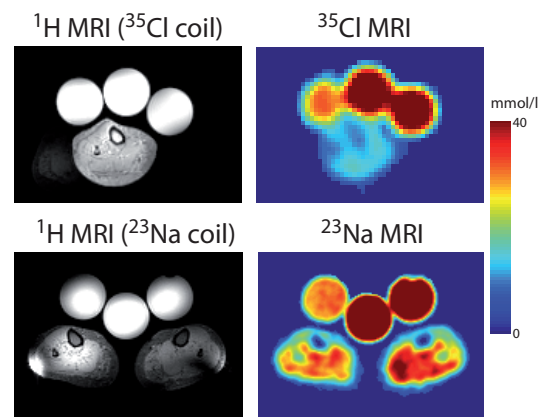


Fig. 3: ^{35}Cl and ^{23}Na MRI of a patient with hypokalemic periodic paralysis. For comparison ^1H MRI data is presented. **^{35}Cl MRI:** Only the right lower leg was examined. The presented image ($\text{TE} = 0.35$ ms) already exhibits T_2^* weighting. The apparent Cl^- concentration is 13 ± 2 mmol/l. Bi-exponential fitting revealed a Cl^- concentration of 18 ± 2 mmol/l. **^{23}Na MRI:** The average Na^+ concentration of the right lower leg is 26.6 ± 0.5 mmol/l.